Crystal Growth and Magnetic Measurements on Aligned Single Crystals of the Oxides Sr_3NiPtO_6 and Sr_3CuPtO_6

John B. Claridge, Ralph C. Layland, W. Hampton Henley, and Hans-Conrad zur Loye*

Department of Chemistry and Biochemistry, University of South Carolina, Columbia, South Carolina 29208

Received December 30, 1998. Revised Manuscript Received March 8, 1999

Crystals of Sr_3NiPtO_6 and Sr_3CuPtO_6 were grown from a K_2CO_3 flux containing $SrCO_3$, NiO or CuO, and Pt metal powder, at 1150 °C. The structure of Sr_3NiPtO_6 was solved by means of single-crystal X-ray diffraction analysis. The structure was refined in space group $R\bar{3}c$, with $a = 9.5832(1)$ Å and $c = 11.1964(1)$ Å. Sr_3CuPtO_6 and Sr_3NiPtO_6 are structurally related to the parent compound, A_4PtO_6 (A = Ca, Sr, Ba), and contain infinite chains of alternating, face-sharing PtO_6 octahedra and $A'O_6$ (A′ = Ni, Cu) trigonal prisms. Magnetic measurements were carried out on both samples using 3−5 mm long single crystals. Magnetic susceptibility studies on oriented single crystals of Sr_3NiPtO_6 indicate the presence of Ni(II) ions with a large single-ion anisotropy ($D = 93.7(5)$ K, $g_{\|} = 2.143(6)$, and $g_{\perp} = 2.392(4)$). In contrast, Sr_3CuPtO_6 exhibits $S = {}^1/_2$ Heisenberg linear chain antiferromagnetism with $J/k = -24.7(1)$ K, $J'/k = -7.3(8)$ K, $g_{\|} = 2.127(6)$, and $g_{\perp} = 2.150(6)$.

Introduction

Oxides of the K_4CdCl_6 structure type (general formula $A_3A'BX_6$) have attracted considerable interest in recent years because of their interesting structure and intriguing magnetic properties.[1−4] The K_4CdCl_6 structure consists of infinite $[A'BX_6]_\infty$ chains consisting of alternating face-sharing octahedra and trigonal prisms; these transition metal containing chains are separated by chains of A cations.[5] Due to the highly anisotropic structure of these oxides, it is desirable to obtain information about the magnetic behavior in fields applied along discrete crystallographic orientations, such as parallel and perpendicular to the transition metal containing chains. Measurements performed on powders, because of the random orientation of the crystallites, can only be used to extract average values of certain magnetic parameters such as the Landé factors. Therefore, to better measure and understand the physical properties of these materials, single crystals large enough to be used in magnetic measurements, are highly desirable. To date, however, most of these systems have only been synthesized as powders, or as crystals too small for physical measurements. Consequently, it has not been possible to obtain detailed information on the magnetic interactions for this class of low-dimensional oxides.

While the synthesis of crystals large enough for physical measurements has not been reported in the literature, the preparation of single crystals suitable for single-crystal analysis of K_4CdCl_6-related oxides, such as Ca_3NaRuO_6,[6] Ca_3NaIrO_6,[6] Sr_3NaRhO_6,[7] Sr_3LiRhO_6,[7] Sr_3LiBiO_6,[8] and Ba_3NaBiO_6,[8] as well as large crystals of barium copper platinum oxides,[9] has been reported. These crystals were typically grown from basic alkali fluxes, e.g. (K,Na)OH,[8] K_2CO_3,[9] and Na_2CO_3.[6] We have, consequently, been investigating the flux growth of $Sr_3A'BO_6$ and related oxides from K_2CO_3 fluxes for the purpose of growing single crystals large enough for carrying out physical measurements.[10]

In this paper, we report the crystal growth and magnetic properties of $Sr_3A'PtO_6$ (A′ = Cu, Ni) and the single-crystal structure of Sr_3NiPtO_6. The single-crystal structure of Sr_3CuPtO_6 has been previously reported,[11] in a monoclinic distortion of the K_4CdCl_6 structure. For both Sr_3NiPtO_6 and Sr_3CuPtO_6, considerably more information about the magnetic interactions can be obtained from magnetic measurements on aligned single crystals than from measurements on randomly oriented powder samples, which have been published previously by us.[2]

* To whom correspondence should be addressed. E-mail: hanno@psc.sc.edu. Telephone: (803) 777-6916.

(1) Nguyen, T. N.; Lee, P. A.; zur Loye, H.-C. *Science* **1996**, *271*, 489.
(2) Nguyen, T. N.; Giaquinta, D. M.; zur Loye, H.-C. *Chem. Mater.* **1994**, *6*, 1642.
(3) Nguyen, T. N.; zur Loye, H.-C. *J. Solid State Chem.* **1995**, *117*, 300.
(4) Kagayama, H.; Yoshima, K.; Kosuge, K.; Mitamura, H.; Goto, T. *J. Phys. Soc. Jpn.* **1997**, *66*, 1607.
(5) Bergerhoff, G.; Schmitz-Dumont, O. *Z. Anorg. Allg. Chem.* **1956**, *284*, 10.
(6) Layland, R. C.; Claridge, J. B.; Adams, R. D.; zur Loye, H.-C. *Z. Anorg. Allg. Chem.* **1997**, *623*, 1131.
(7) Reisner, B. A.; Stacy, A. M. *J. Am. Chem. Soc.* **1998**, *120*, 9682.
(8) Carlson, V. A.; Stacy, A. M. *J. Solid State Chem.* **1992**, *96*, 332.
(9) Chen, Z.; Qian, Y.; Wu, Y.; Sun, D.; Lin, R.; Cheng, T.; Niu, L.; Zhou, G.; He, Z.; Xia, J.; Zao, Y.; Zhang, Q. *J. Cryst. Growth* **1989**, *94*, 277.
(10) Claridge, J. B.; Henley, W. H.; Smallwood, P. L.; zur Loye, H.-C. *J. Cryst. Growth*, in print.
(11) Hodeau, J. L.; Tu, H. Y.; Bordet, P.; Fournier, T.; Strobel, P.; Marezio, M.; Chandrashekhar, G. V. *Acta Crystallogr.* **1992**, *B48*, 1.
(12) *International Tables for Crystallography*; Kynoch Press: Birmingham, England, 1975; Vol. IV, Table 2.2B.
(13) *International Tables for Crystallography*; Kynoch Press: Birmingham, England, 1975; Vol. IV, Table 2.3.1.

10.1021/cm9811592 CCC: $18.00
Published on Web 04/20/1999

Experimental Section

Sample Preparation. Single crystals were grown out of a flux of reagent grade K_2CO_3 using $SrCO_3$ (Alfa, 99.99%), NiO (Alfa, 99.998%), CuO (Alfa, 99.999%), and Pt (Engelhard, 99.95%) as reagents. The mixture was heated at a rate of 10 °C/min to 1050 °C, held at that temperature for 72 h, and then cooled at a rate of 0.2 °C/min to 880 °C, at which point the flux has solidified. The flux was removed by washing with water, and black crystals of $Sr_3A'PtO_6$ (A′ = Ni, Cu) were isolated. The crystals were further cleaned by sonication to remove any remaining flux matrix. Several crystals, suitable for single-crystal X-ray diffraction analysis, were selected under a polarized light microscope. Larger crystals used for magnetic measurements were grown by increasing the temperature to 1150 °C and by slowing down the cooling rate to 0.1 °C/min.

Single-Crystal Structure Determination. A pseudo-hexagonal rod-shaped (0.2 × 0.2 × 0.6 mm in size) crystal of Sr_3NiPtO_6 was selected. The crystal used for the intensity measurements was mounted in a thin-walled glass capillary. Diffraction measurements at 20 °C were made on a Rigaku AFC6S four-circle diffractometer using Mo Kα radiation. The unit cell was determined from 25 randomly selected reflections obtained by using the AFC6 automatic search, center, index, and least-squares routines. Crystal data, data collection parameters, and the results of the analysis for Sr_3NiPtO_6 are listed in Table 1. All data processing was performed on a Silicon Graphics INDIGO[2] computer by using the TEXSAN structure-solving program library obtained from the Molecular Structure Corp. (The Woodlands, TX). Lorentz−polarization (*Lp*) and an absorption correction were applied to the data. Neutral atom scattering factors were calculated by the standard procedures.[12] Anomalous dispersion corrections were applied to all atoms.[13] Full-matrix least-squares refinements minimized the function:

$$\sum_{hkl} w(|F_o| - |F_c|)^2$$

where $w = 1/\sigma(F)^2$, $\sigma(F) = \sigma(F_o^2)/2F_o$, and $\sigma(F_o^2) = [\sigma(I_{raw})^2 + (0.02I_{net})^2]^{1/2}/Lp$. The intensities of three standard reflections were measured every 150 reflections. These reflections showed no significant deviations during the data collection process.

The compound Sr_3NiPtO_6 crystallized in the rhombohedral crystal system. The patterns of systematic absences observed in the data were consistent with either the space groups $R3c$ or $R\bar{3}c$. The centric space group, $R\bar{3}c$, was assumed and confirmed by the successful solution and refinement of the structures. The structure was solved by a combination of direct methods (MITHRIL) and difference Fourier syntheses. All atoms were refined with anisotropic thermal parameters.

Magnetic Measurements. The magnetic susceptibilities of $Sr_3A'PtO_6$ (A′ = Ni, Cu) were measured using a Quantum Design MPMS XL SQUID magnetometer in applied fields of 5 and 40 kOe. The unit cells of the crystals which were used for the magnetic measurements were confirmed by X-ray diffraction analysis. Large single crystals of $Sr_3A'PtO_6$ (A′ = Ni, Cu) (4 and 2.5 mm long and weighing 16.02 and 1.14 mg, respectively) were mounted on plastic straws using Capton tape. The straw and Capton tape covered the entire scanned region in order to minimize the sample holder contribution. The magnetization of each single crystal was measured in both a parallel and perpendicular orientation relative to the applied magnetic field. The parallel orientation refers to the alignment of the chain direction (or *c* axis) parallel to the applied field. The samples were loaded at room temperature, and measurements were taken in the temperature range 2 K ≤ *T* ≤ 300 K after cooling the sample in zero magnetic field (zero-field cooled, ZFC) and also after cooling in the measuring field (field cooled, FC). For clarity in the figures, only the magnetic data from 2 to 150 K are plotted.

Scanning Electron Microscopy. The scanning electron micrographs were obtained using a Hitachi 2500 Delta scanning electron microscope. The surface of the crystals was coated with gold or carbon to prevent charging.

Table 1. Crystallographic Data for Sr_3NiPtO_6

formula	Sr_3NiPtO_6
formula weight	612.65
crystal system	trigonal
lattice parameters	
a (Å)	9.5832(1)
c (Å)	11.1964(1)
V (Å^3)	890.492(9)
space group	$R\bar{3}c(h)$ (no. 167)
Z value	6
μ(Mo Kα) (cm^{-1})	532.08
temp (°C)	20.0
2θ max (deg)	70.0
no. of obsns ($I > 3\sigma$)	214
no. of variables	20
goodness of fit	2.140
residuals: *R*; R_w[a]	0.041; 0.050
absorption corrn	DIFABS
min/max	0.422/1.000

[a] $R = \sum_{hkl}(||F_{obs}| - |F_{calc}||/\sum_{hkl}|F_{obs}|$; $R_w = [\sum_{hkl} w(|F_{obs}| - |F_{calc}|^2)/\sum_{hkl} wF_{obs}^2]^{1/2}$, $w = 1/\sigma^2(F_{obs})$; GOF $= [\sum_{hkl} w(|F_{obs}| - |F_{calc}|)^2/(n_{data} - n_{vari})]^{1/2}$.

Results and Discussion

Crystals of $Sr_3A'PtO_6$ (A′ = Ni, Cu) were grown in K_2CO_3 melts at temperatures ranging from 1050 to 1150 °C. The highest quality crystals were obtained at 1050 °C followed by cooling to 800 °C at 0.2 °C/min. These small crystals were used for the single-crystal structural analysis. Heating the flux to 1150 °C followed by cooling to 800 °C at 0.1 °C/min leads to the formation of large single crystals, some as long as 5 mm in their longest dimension. In general, the crystals of Sr_3NiPtO_6 were larger and had smaller aspect ratios than those of Sr_3CuPtO_6. SEM pictures of crystals of Sr_3NiPtO_6 and Sr_3CuPtO_6 are shown in Figure 1. The pseudo-hexagonal habit of the crystals is clearly visible in the photographs. For the monoclinic Sr_3CuPtO_6, this hexagonal habit is due to a strong pseudo-rhombohedral metric symmetry, leading to significant twinning along the pseudo-hexagonal [001] as demonstrated by Hodeau et al.[11]

Crystallographic data for the single crystal of Sr_3NiPtO_6 are given in Table 1. The atomic positions and thermal parameters for Sr_3NiPtO_6 can be found in Table 2. Selected interatomic bond distances and angles can be found in Table 3. Sr_3NiPtO_6 is isostructural with the rhombohedral structure type K_4CdCl_6, as was expected on the basis of the fairly large number of compounds that have been synthesized with this structure type. Sr_3CuPtO_6 forms in a monoclinic distortion of the K_4CdCl_6 structure type.[5] The rhombohedral structure can be described as consisting of chains of alternating face-sharing trigonal prisms and octahedra. A view of the unit cell looking down [001] can be seen in Figure 2. In the monoclinic modification, the copper atoms move from the center of the trigonal prisms to their faces, thereby taking on a pseudo-square planar coordination. A comparison between the two types of chains is shown in Figure 3. The strontium ions are coordinated in a distorted square antiprism by eight oxygens in a range of 2.48(1)−2.73(1) Å. The platinum ions are located at the corners and center of the unit cell. Six equivalent oxygen ions are coordinated to the platinum ion in an octahedral array at distance of 2.01(1) Å. The Pt−O

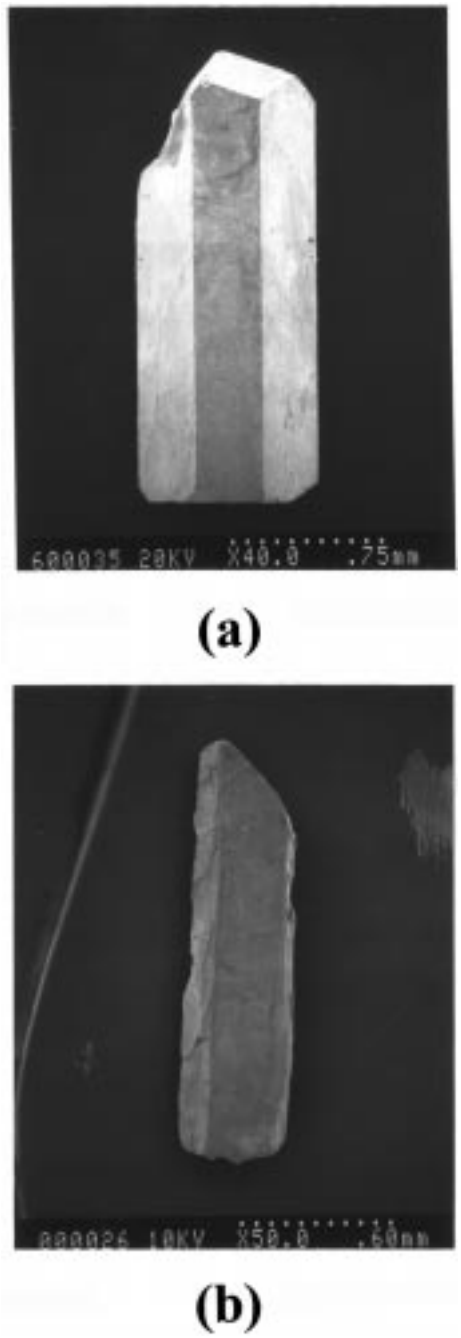

Figure 1. SEM micrographs of (a) Sr_3NiPtO_6 and (b) Sr_3CuPtO_6 single crystals showing clearly the pseudo-hexagonal habit of the crystals.

Table 2. Atomic Positions and Isotropic Thermal Parameters with Esds (in Parentheses) for Sr_3NiPtO_6

compd	atom	site	*x*	*y*	*z*	**B**
Sr_3NiPtO_6	Sr	18 e	0.3644(2)	0	1/4	0.30(2)
	Ni	6 a	0	0	1/4	0.44(3)
	Pt	6 b	0	0	0	0.13(1)
	O	36 f	0.174(1)	0.023(1)	0.1128(8)	0.6(2)

bond distances are in agreement with those found for Pt(IV) in other structurally related oxides.[11,14−16] The nickel metal ions are also located at the corners and center of the unit cell and are coordinated in a trigonal prismatic array by six equivalent oxygen ions at a distance of 2.19(1) Å. To verify that the nickel site was fully occupied, the occupancy of the nickel atom was refined and found to be within experimental error of being fully occupied. Therefore the occupancy of the nickel atom was set back to fully occupied and not refined further. The trigonal prisms are distorted by a twist about the 3-fold axis (ϕ) of 14.0(1)°.

Magnetic measurements of Sr_3CuPtO_6 and Sr_3NiPtO_6 were carried out on oriented crystals in the temperature

Table 3. Interatomic Distances (Å) and Bond Angles (deg) with Esds (in Parentheses) for Sr_3NiPtO_6.

atom	atom	distance		atom	atom	atom	angle	
Pt	Sr	3.1958(6)	(×6)	Pt	O	Ni	83.4(4)	
Pt	Ni	2.8001(6)	(×2)	O	Pt	O	84.7(4)	(×6)
Pt	O	2.01(1)	(×6)	O	Pt	O	95.3(4)	(×6)
Sr	O	2.48(1)	(×2)	O	Pt	O	180	(×3)
Sr	O	2.605(9)	(×2)	O	Ni	O	76.3(4)	(×6)
Sr	O	2.66(1)	(×2)	O	Ni	O	89.9(5)	(×3)
Sr	O	2.73(1)	(×2)	O	Ni	O	129.0(4)	(×3)
Ni	O	2.19(1)	(×6)	O	Ni	O	147.8(5)	(×3)

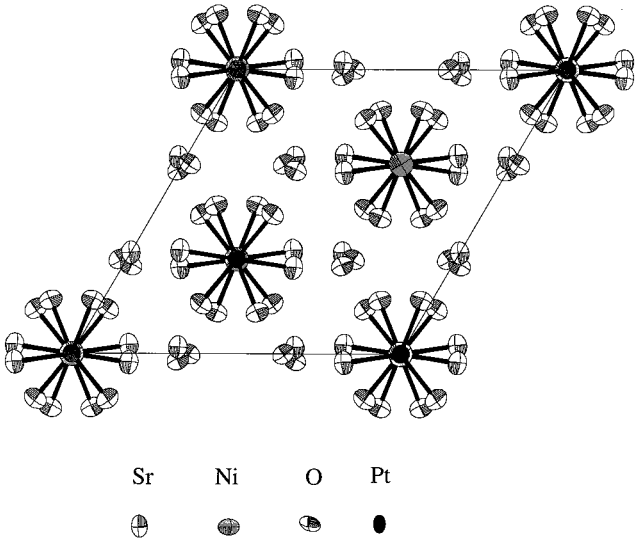

Figure 2. Structure of Sr_3NiPtO_6 viewed along [001].

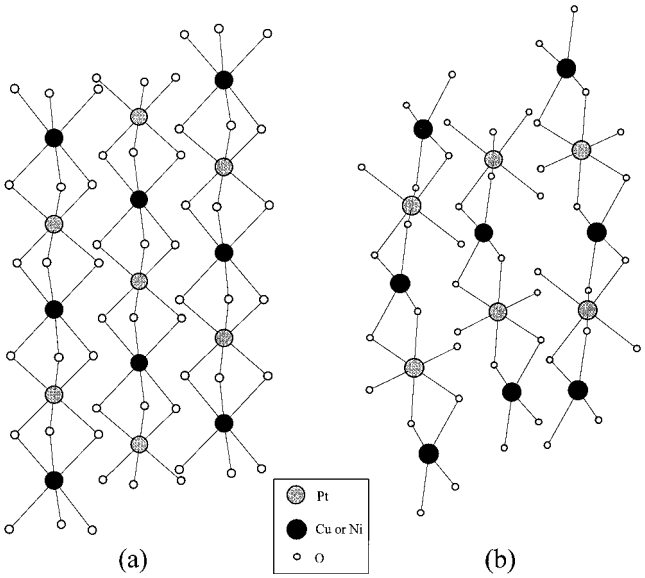

Figure 3. Comparison of the $[A'PtO_6]_\infty$ chains in Sr_3NiPtO_6 (a) and Sr_3CuPtO_6 (b).

(14) Tomaszewska, A.; Müller-Buschbaum, Hk. *Z. Anorg. Allg. Chem.* **1992**, *617*, 23.
(15) Wilkinson, A. P.; Cheetham, A. K. *Acta Crystallogr.* **1989**, *C45*, 1672.
(16) Randall, J. J.; Katz, L. *Acta Crystallogr.* **1959**, *12*, 519.

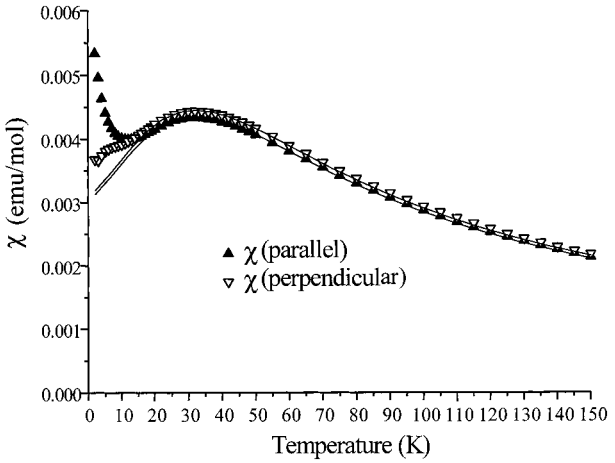

Figure 4. Temperature dependence of the susceptibility of Sr_3CuPtO_6 with **H**⊥**[201]** and **H**||**[201]**. The solid lines correspond to the fit.

range of 2 K ≤ T ≤ 300 K to obtain information concerning the magnetic behavior parallel and perpendicular to the transition metal chains direction. Since two sets of magnetic data were collected for each compound, the data could be fit better to available magnetic models and more information could be obtained than from similar measurements and fits carried out on powder samples.

Figure 4 shows the temperature dependence of the magnetic susceptibility for Sr_3CuPtO_6 measured parallel and perpendicular to the pseudo-hexagonal c axis following subtraction of the temperature-independent component. The ratio $\chi_{||}/\chi_{\perp}$ is constant in the temperature range T > 20 K, indicating that the anisotropy in this temperature range is due to the ratio of the Landé factors $g_{||}/g_{\perp}$. The most prominent features in the susceptibility are a broad maximum at $T \sim 32$ K and a divergence between the parallel and perpendicular measurements below 20 K. The first of these features is indicative of some form of short-range antiferromagnetic order. Given the obvious structural motif of $[CuPtO_6]_\infty$ chains in the structure it is tempting to think of this as being due to some form of 1-D chain type interaction. Therefore, the data were fitted to the expressions derived by Hatfield[17] from the work of Bonner and Fischer,[18] for a linear Heisenberg $S = {}^1/_2$ chain with and without interchain coupling (eqs 1 and 2, respectively), which are valid for $kT/|J| \geq 0.5$ (where $x = |J|/kT$, $A = 0.25$, $B = 0.14995$, $C = 0.30094$, $D = 1.9862$, $E = 0.68854$, $F = 6.0626$, and z is the number of interchain nearest neighbors, taken as 2 in this case):

$$\chi_H = \frac{Ng^2\mu_B{}^2}{kT}\frac{A + Bx^{-1} + Cx^{-2}}{1 + Dx^{-1} + Ex^{-2} + Fx^{-3}} \qquad (1)$$

$$\chi = \chi_H/(1 - 2zJ'\chi_H/Ng^2\mu_B{}^2) \qquad (2)$$

Both models fit the data well above 20 K. However, given the fact that the interchain $Cu^{2+}-Cu^{2+}$ distances ($2 \times 5.146(3)$ and $2 \times 5.902(3)$ Å) are on the order of or shorter than the intrachain distances ($2 \times 5.719(3)$ Å), the second model would appear to be more realistic and, therefore, is the fit shown in Figure 4. The deviation in the magnetic susceptibility for the copper compound below 20 K can be attributed to the fact that the model is only valid above $2kT > J$, a condition which does not hold at low temperatures. Also, it is likely that the compound is beginning to order magnetically in three dimensions, causing the deviation from the model. The parameters obtained from the fit of the magnetic data using eq 2 are $J/k = -24.7(1)$ K, $J'/k = -7.3(8)$ K, $g_{||} = 2.127(6)$, and $g_{\perp} = 2.150(6)$. The ratio of the intrachain and interchain coupling constants is $J/J' \sim 3$, indicating that, while the intrachain coupling is stronger than the interchain coupling, there is nonetheless a significant interchain coupling present. Consequently, the system should not be considered to be magnetically one-dimensional.

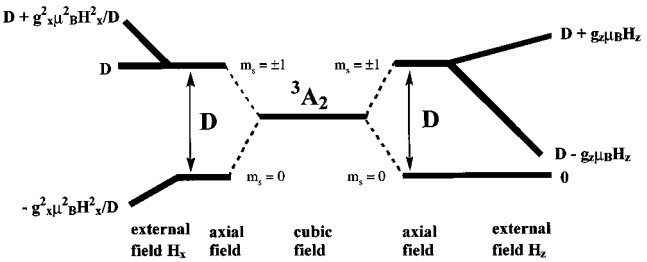

Figure 5. Splitting of nickel(II) with an internal axial field and an external magnetic field (adapted from ref 19).

As previously reported, the magnetic properties of polycrystalline powders of Sr_3NiPtO_6 were described in terms of noninteracting ions with a large single-ion anisotropy (D).[2] This model is discussed in more detail by Carlin[19] and, therefore, it will only be summarized here. The axial crystal field splits the $^3A_2$ free ion ground state into $m_s = 0$ and $m_s = \pm 1$ components with a separation D. In an applied magnetic field these terms are further split, as shown schematically in Figure 5, for applied fields both perpendicular and parallel to the anisotropy axis, H_x and H_z, respectively. Using this model it is possible to derive the equations for the magnetic susceptibilities with the measuring field parallel (eq 3) and perpendicular (eq 4) to the principal axis.

$$\chi_{||} = \frac{2Ng_{||}{}^2\mu_B{}^2}{kT}\frac{e^{-D/kT}}{(1 + 2e^{-D/kT})} \qquad (3)$$

$$\chi_{\perp} = \frac{2Ng_{\perp}{}^2\mu_B{}^2}{3kT}\frac{6kT}{D}\left(\frac{1 - e^{-D/kT}}{1 + 2e^{-D/kT}}\right) \qquad (4)$$

Figure 6 shows the magnetic susceptibility for Sr_3NiPtO_6 measured parallel (**H**||**c**) and perpendicular (**H**⊥**c**) to the hexagonal c axis together with the best fit to the model detailed above. The fit parameters are as follows: $D/k = 93.7(5)$ K, $g_{||} = 2.143(6)$, and $g_{\perp} = 2.392(4)$. As can be seen in Figure 6 the model fits the susceptibility very well. A good fit is obtained for **H**⊥**c** over the entire data range, while for **H**||**c**, deviations between the data and the fit can be noticed starting at about 30−40 K. The value of D/k obtained is very large when compared with those obtained for molecular nickel complexes, for which D/k values are typically on the

(17) Hatfield, W. E. *J. Appl. Phys.* **1981**, *52*, 1985.

(18) Bonner, J. C.; Fischer, M. E. *Phys. Rev.* **1964**, *A135*, 640.

(19) Carlin, R. L. *Magnetochemistry;* Springer-Verlag: Berlin Heidelberg 1986; p 21.

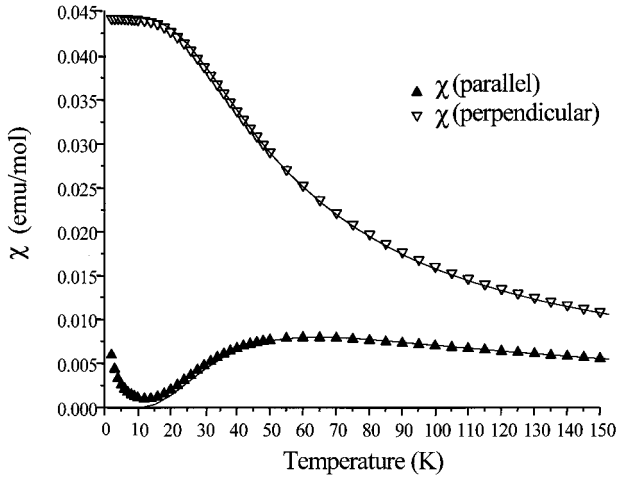

Figure 6. Temperature dependence of the susceptibility of Sr_3NiPtO_6 with **H**⊥**c** and **H**||**c**. The solid lines correspond to the fit.

order of a few degrees. However, when we compare Sr_3NiPtO_6 with other structurally distorted systems, such as NiX_2L_2 (X = Cl, Br; L = pyridine, pyrole; $D/k \sim -30$ K),[20] BaY_2NiO_5 ($D/k = 46$ K),[21] and the 2-H perovskite-type $AFeX_3$ halides (A = Cs, Rb; X = Cl, Br; 12 K < D/k < 76 K),[22] which behave as fictitious $S = 1$ systems, then the value of D/k is not unreasonably large.

Below 40 K, the magnetic susceptibility measured with **H**||**c** deviates significantly from that expected based on the single-ion anisotropy model, and furthermore, the value of the magnetic susceptibility shows an applied field dependence.

As can be seen from Figure 7a, even at 5 K with **H**⊥**c**, the plot of M vs H is linear, indicating that there is no hint of ferromagnetic or antiferromagnetic ordering. However, when **H**||**c**, the behavior is very different and the M vs H plot displays a considerable history dependence and an apparent saturation of the moment at an applied field of about 40 kOe. The origin of this magnetic order is not understood at the present time. However, similar magnetic behavior has been observed in the $AFeX_3$ 2-H perovskite-type systems mentioned above. For such singlet ground-state systems long-range magnetic order does not occur when the exchange interaction between neighboring ions is much smaller than the excitation of an ion to its magnetic levels.[23] As shown in Figure 5, in an applied field, the $m_s = -1$ state is lowered in energy relative to the ground state. In addition, coupling interactions also lower the energy of the $m_s = -1$ state relative to the $m_s = 0$ state.[24] Thus, for Sr_3NiPtO_6, no ordering is apparent in low-field susceptibility measurements, while in the 40 kOe measurements and M vs H measurements, there appears to be long-range ordering at finite fields. To confirm or disprove that such a behavior exists in Sr_3NiPtO_6, physical techniques other than susceptibility measurements would be required.

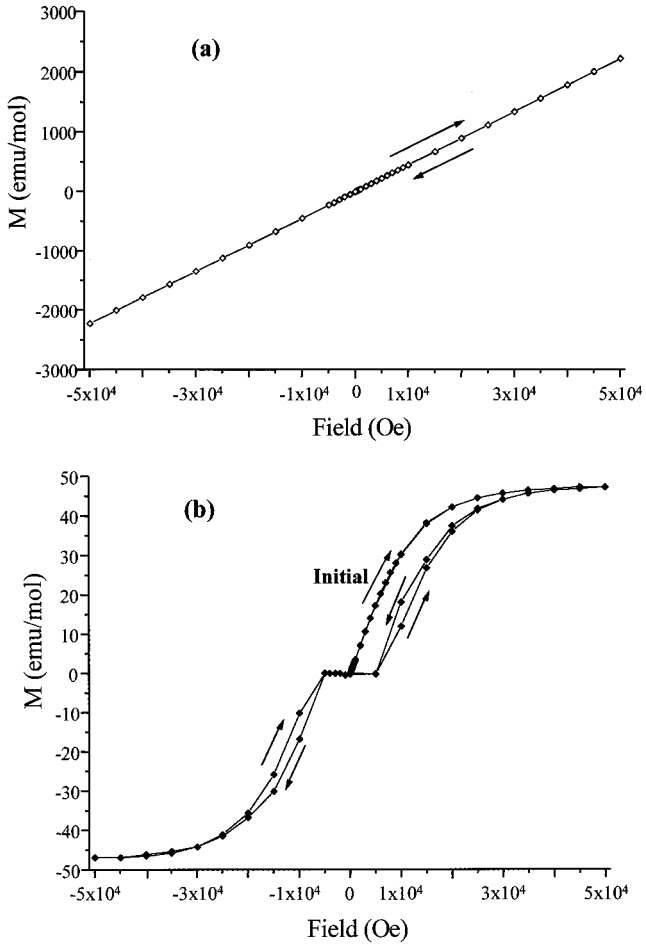

Figure 7. Magnetization vs applied magnetic field data for Sr_3NiPtO_6 measured at 5 K with (a) **H**⊥**c** and (b) **H**||**c**.

In conclusion, crystals of the oxides Sr_3NiPtO_6 and Sr_3CuPtO_6, suitable for single-crystal structural investigation and aligned magnetic measurements, can be grown from K_2CO_3 fluxes. Aligned magnetic measurements on Sr_3NiPtO_6 and Sr_3CuPtO_6 crystals show that the former can be thought of as a singlet ground-state system while the later is a $S = {}^1/_2$ Heisenberg chain, albeit with a large interchain coupling constant.

Acknowledgment. Financial support was provided by the National Science Foundation through Grant No. DMR 9696235. The authors also thank Dr. Richard D. Adams for the use of his single-crystal X-ray diffractometer. The SQUID magnetometer was purchased from funds provided by the CRIP program of the NSF (CHE-9700019).

Supporting Information Available: Tables of crystallographic data, structure factor tables, interatomic bond distances and angles, and anisotropic thermal parameters for Sr_3NiPtO_6. This material is available free of charge via the Internet at http://pubs.acs.org.

CM9811592

(20) Klaaijsen, F. W.; Dokoupil, Z.; Huiskamp, W. J. *Physica* **1975**, *79B*, 457.
(21) Darriet, J.; Regnault, L. P. *Solid State Commun.* **1993**, *86*, 409.
(22) Collins, M. F.; Petrenko, O. A. *Can. J. Phys.* **1997**, *75*, 605 and references therein.
(23) Teuneto, T.; Murao, H. *Physica* **1971**, *51*, 186.
(24) Chiba, M.; Ajiro, Y.; Adachii, K.; Morimoto, T. *J. Phys. Soc. Jpn.* **1988**, *57*, 3178.